

Characteristics and Design of Broadside-Coupled Transmission Line at a Higher Order Leaky Mode

Kuo-Feng Steve Huang, *Student Member, IEEE*, and Ching-Kuang C. Tzuang, *Fellow, IEEE*

Abstract—The aim of this paper is to provide: 1) a detailed description of the higher order leaky modes of the much-used broadside-coupled microstrips and 2) demonstrate the practical application of such leaky modes as an antenna. A representative broadside-coupled transmission-line structure is examined to elucidate the detail of leakage effects at higher order of multilayered three-dimensional microwave and millimeter-wave circuits. Two-layer cases are analyzed from a physical perspective and the total number of first higher order leaky modes is found to be equal to that of microstrips.

One of the two first higher order leaky modes obtained in the two-layer case is weakly attenuated, while the other is strongly attenuated. A high-gain narrow-beam leaky-mode antenna using only the weakly attenuated leaky mode is designed and measured as an application of this broadside-coupled structure, exhibiting a marked beamwidth reduction of 60%. This antenna is the first Yagi-Uda-like array antenna that utilizes the higher order leaky modes of the microstrip, for which the three basic elements—driver, reflector, and director—are stacked in the broadside direction. The attenuation rate can be further reduced by adjusting the strip width of the director. The half-power beamwidth of the leaky-mode antenna applying two-layer broadside-coupled microstrips with a wider top microstrip is measured to be 2.10° at 25.20° from the broadside at 34 GHz.

Index Terms—Antenna arrays, high gain, multilayered, narrow beam.

I. INTRODUCTION

ROADSIDE-COUPLED line structures have been comprehensively investigated and extensively applied in recent decades [1]–[6]. This structure makes circuits more compact and flexible, and is naturally adaptable to multilayered structures. Despite limited knowledge of higher order effects, the analyses of these structures focus primarily on the dominant bound modes and do not address the potential leaky properties when the layered integrated circuits are partially or completely open.

A few studies consider the zero-cutoff leaky modes in a transversely open symmetric structure with an air gap in the form of surface waves [7]. Apart from these companion types of modes, which are leaky, but carry dominant-mode-like modal currents [8], the higher order leaky modes on the completely open broadside-coupled microstrips embedded in the stratified substrates above a common ground plane have recently been

Manuscript received October 15, 2001; revised April 17, 2002. This work was supported in part by the Ministry of Education of Taiwan under Grant 89-E-FA06-2-4.

The authors are with the Department of Communication Engineering, National Chiao Tung University, Hsinchu, Taiwan, R.O.C. (e-mail: cktzuang@cc.nctu.edu.tw).

Digital Object Identifier 10.1109/TMTT.2002.807839

reported [9]. This study found that the number of first higher order leaky modes (EH_1) equals the total number of microstrips (excluding the ground plane). This result is consistent with the coupled-mode theory applied in parallel-coupled microstrips at higher order [10].

One most common application of microstrips at higher order is the leaky-mode antenna, which is quite suited to planar realization [11]–[13]. The radiation performance of the leaky-mode antenna is known to depend strongly on the complex propagation constant $\gamma = \beta - j\alpha$, where β is the phase constant and α is the attenuation (leaky) constant. The beam-angle θ_m (angle of the radiation main beam from broadside) can be determined directly from $\beta(\theta_m) \approx \sin^{-1}(\beta/k_o)$ [11] in case α is small; hence, the leaky-mode antenna has the ability of frequency scanning.

The value of α is related to the directivity of the leaky-mode antenna. The radiation pattern of the leaky microstrip can be established using the equivalent-surface magnetic-current method [14]. If the leaky-mode antenna is long enough to radiate above 90% of its power, then the half-power beamwidth in elevation can be simply represented as [14]

$$\theta_{3\text{ dB}} \cong \frac{\alpha/k_o}{0.183 \cdot \cos \theta_m}. \quad (1)$$

Equation (1) shows that the half-power beamwidth in elevation becomes much wider as the radiation main-beam approaches the end side (i.e., $\theta_m \rightarrow 90^\circ$). However, α comes to dominate the radiation beamwidth since the cosine function is relatively flat over $0^\circ < \theta_m < 45^\circ$. As shown in this equation, $\theta_{3\text{ dB}}$ is almost directly proportional to α , especially when θ_m approaches the broadside (i.e., $\theta_m \rightarrow 0^\circ$). Restated, the antenna beamwidth falls and the directivity of the antenna rises as the attenuation constant α decreases.

Jackson and Oliner [15] and Jackson *et al.* [16] stated that the excitation of weakly attenuated leaky waves contributes to the antenna gain enhancement of a multiple-layer dielectric structure. These weakly attenuated leaky waves can also exist in many dielectric waveguide structures with periodic perturbations [17]–[19]. Such leaky structures, showing genuine adjustments in the size and period of perturbation, can achieve small α when the radiation main beam is still far from the end side; high-gain narrow-beam leaky-wave antennas can thus be realized. The antenna described in [17] is electrically long (approximately $300 \lambda_0$) and the normalized attenuation constant (α/k_0 , where $k_0 = 2\pi/\lambda_0$, λ_0 is the free-space wavelength) is approximately 0.0006 at 90 GHz when the radiation main beam scans from 20° to 30° from the broadside.

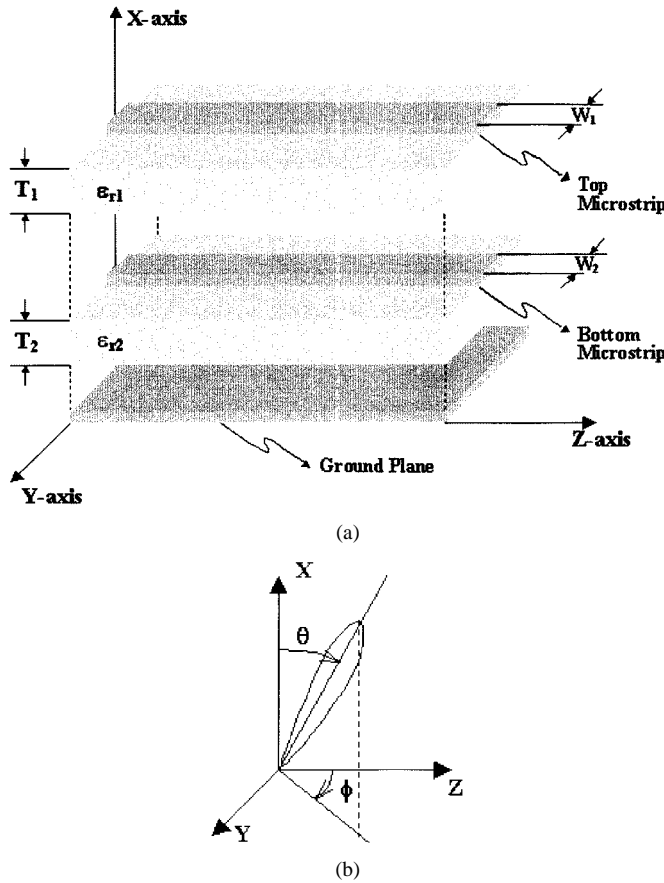


Fig. 1. (a) Proposed two-layer broadside-coupled microstrips. The width $W_1 = W_2 = W$ of either microstrips is 2.5 mm, the thickness $T_1 = T_2 = T$ of the substrates is 0.254 mm, and the relative dielectric constant $\epsilon_{r1} = \epsilon_{r2} = \epsilon_r$ is 3.0. Both microstrips of infinite length are centered at the Y -axis. (b) Coordination system.

This paper presents a new leaky-mode antenna that applies two-layer broadside-coupled microstrips, as shown in Fig. 1; the antenna can also achieve a low attenuation rate. The antenna can be easily integrated with the RF front-end circuits using a conventional printed circuit board (PCB) fabrication process, as the broadside-coupled structure is natively planar and multilayered. In these two-layer broadside-coupled microstrips, the attenuation constant α for one of the two EH_1 modes falls after coupling in relation to corresponding values of β . That is, the reported leaky-mode antenna can be electrically long and the antenna gain can be enhanced by decreasing θ_{3dB} . For this weakly attenuated EH_1 mode, the current flowing on the top microstrip is lower in magnitude and opposite in direction to the current flowing on the bottom microstrip.

Array theory [20] dictates that the radiation of this array antenna is *directed* from the bottom microstrip toward the top microstrip. Furthermore, the energy radiated from these two microstrips is completely *reflected* from the ground plane, yielding a single beam. Thus, the reported leaky-mode antenna can be considered as the simplest three-element Yagi–Uda-like array antenna, including a driver (bottom microstrip), reflector (ground plane), and director (top microstrip). As for the typical Yagi–Uda antenna, a better radiation (for higher directivity) can be achieved by controlling the geometric parameters of the two microstrips. Section III demonstrates that a slightly

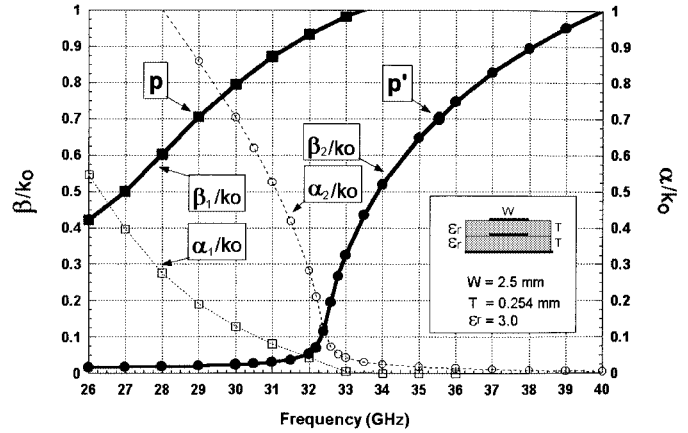


Fig. 2. Normalized phase constants β/k_0 (solid line) and the normalized attenuation constants α/k_0 (dashed line) against frequency of two-layer broadside-coupled microstrips. The γ_1 leaky mode (nearly in-phase) and the γ_2 leaky mode (nearly out-of-phase) are marked with squares and circles, respectively.

wider top microstrip can further reduce α and θ_{3dB} to an extremely low value. In this paper, this weakly attenuated EH_1 mode is purely excited to construct a high-gain narrow-beam leaky-mode antenna.

The remainder of this paper is organized as follows. Section II thoroughly investigates the broadside-coupled transmission line at higher order from the following three perspectives:

- 1) dispersion characteristics;
- 2) modal currents;
- 3) detailed observation of the field distributions.

Section III describes the design procedure of the reported high-gain leaky-mode antenna using broadside-coupled microstrips, as well as the simulated and measured results. Experiments reveal that the reported antenna can control the attenuation rate. Section IV summarizes the results and presents conclusions.

II. CHARACTERISTICS OF TWO-LAYER BROADSIDE-COUPLED MICROSTRIPS

The complicated laterally and multiple multilayered transmission lines are reduced to an inhomogeneous broadside-coupled microstrips structure, as seen in Fig. 1. In this configuration, width, center position, substrate thickness, and substrate dielectric constant for both microstrips are assumed identical for further simplification of the problem. The width $W_1 = W_2 = W$ of either microstrips is 2.5 mm and the thickness $T_1 = T_2 = T$ of the substrates with relative dielectric constant $\epsilon_{r1} = \epsilon_{r2} = \epsilon_r$ of 3.0 is 0.254 mm. The microstrips of infinite length are centered at the Y -axis. Notice that the substrate thickness of 0.254 mm with low dielectric constant of 3.0 is often the choice for millimeter-wave modules and hybrids.

The full-wave integral-equation method is invoked to obtain two leaky modes at the first higher order (EH_1), namely, γ_1 and γ_2 , spanning the whole Ka -band (26–40 GHz), as shown in Fig. 2. A total of two EH_1 leaky modes is searched, confirming our expectation that the number of EH_1 leaky modes should equal that of the microstrips [10].

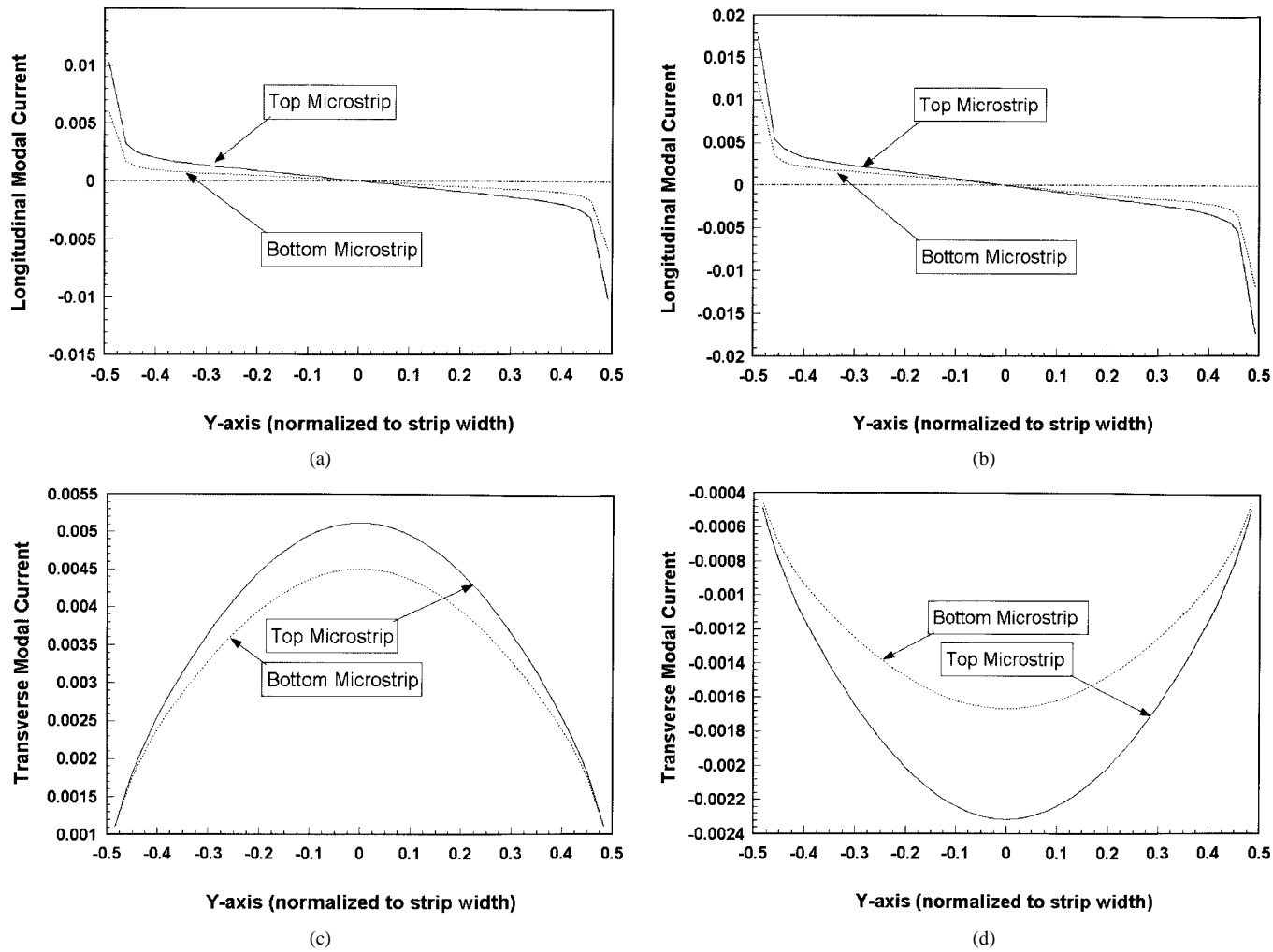


Fig. 3. Modal current distributions of the γ_1 mode on the top (solid line) and bottom (dashed line) microstrips at 31 GHz. The γ_1 modal currents flowing on the top and bottom microstrips are nearly in-phase (with a phase difference of 5.4°) and differ in magnitude by a ratio of 1 : 0.65. (a) The real parts for γ_1 . (b) The imaginary parts for γ_1 . (c) The real parts for γ_1 . (d) The imaginary parts for γ_1 .

Fig. 2 shows the normalized complex propagation constants γ_1/k_0 and γ_2/k_0 , where $\gamma_1 = \beta_1 - j\alpha_1$, $\gamma_2 = \beta_2 - j\alpha_2$, and $k_0 = 2\pi/\lambda_0$. λ_0 is the free-space wavelength. The γ_1 leaky mode occupies the lower Ka -band. Its cutoff frequency begins around 33.5 GHz where the normalized phase constant β_1/k_0 crosses unity and the normalized attenuation constant α_1/k_0 becomes nonzero. The γ_2 mode spans the higher Ka -band, between 33–40 GHz. Together, γ_1 and γ_2 cover the whole Ka -band, representing a bandwidth considerably larger than that of a typical microstrip leaky line at higher order [11]. As shown in Fig. 2, both the distributions of β_1 and α_1 are much flatter than those of β_2 and α_2 . The normalized phase constants β_1/k_0 at point P and β_2/k_0 at P' , as shown in Fig. 2, are both 0.7, where the normalized attenuation constant α_2/k_0 (approximately 0.02) is much lower than α_1/k_0 (approximately 0.19). The value of α_2/k_0 remains below 0.1 over the frequency range of 32.5–40 GHz, when β_2/k_0 increases from 0.1 to 1.0, revealing that γ_2 can establish a wide-band antenna with a great scan range.

Without loss of generality, the modal currents of the γ_1 and γ_2 modes at 31 GHz are verified as being of the EH_1 type, as shown in Figs. 3 and 4, respectively. Both metal strips have

longitudinal (transverse) current distributions that exhibit odd (even) symmetry about the central z - x -plane. The solid lines in the figures all represent the currents that flow on the top microstrip, and the dashed lines represent those on the bottom microstrip. The γ_1 modal currents on the top and bottom microstrips are nearly in-phase (with a phase difference of 5.4°) and out-of-phase (with a phase difference of 186.1°) for the γ_2 mode. Notably, the broadside-coupled structure is inhomogeneous and nonsymmetric in the broadside (x -axis); therefore, the γ_1 and γ_2 modes can not exhibit either even or odd symmetry. Thus, the modal currents on the top and bottom microstrips differ by 35% and 34% in magnitude for the γ_1 and γ_2 modes, respectively. Paralleling to the terminology for bound modes of coupled microstrips, γ_1 and γ_2 , the higher order EH_1 leaky modes, correspond to the β_π and β_c modes, respectively.

The electric and magnetic fields of the γ_1 mode at 29 GHz on the transverse plane ($Z = 0$) are plotted in Fig. 5(a) and (b), and the normalized phase constant (β_1/k_0) is 0.70 at this frequency. Similarly, Fig. 6(a) and (b) illustrates the electric and magnetic field of the γ_2 mode at 34 GHz, where β_2/k_0 is 0.52. Since the fields due to the EH_1 modes are antisymmetric against the

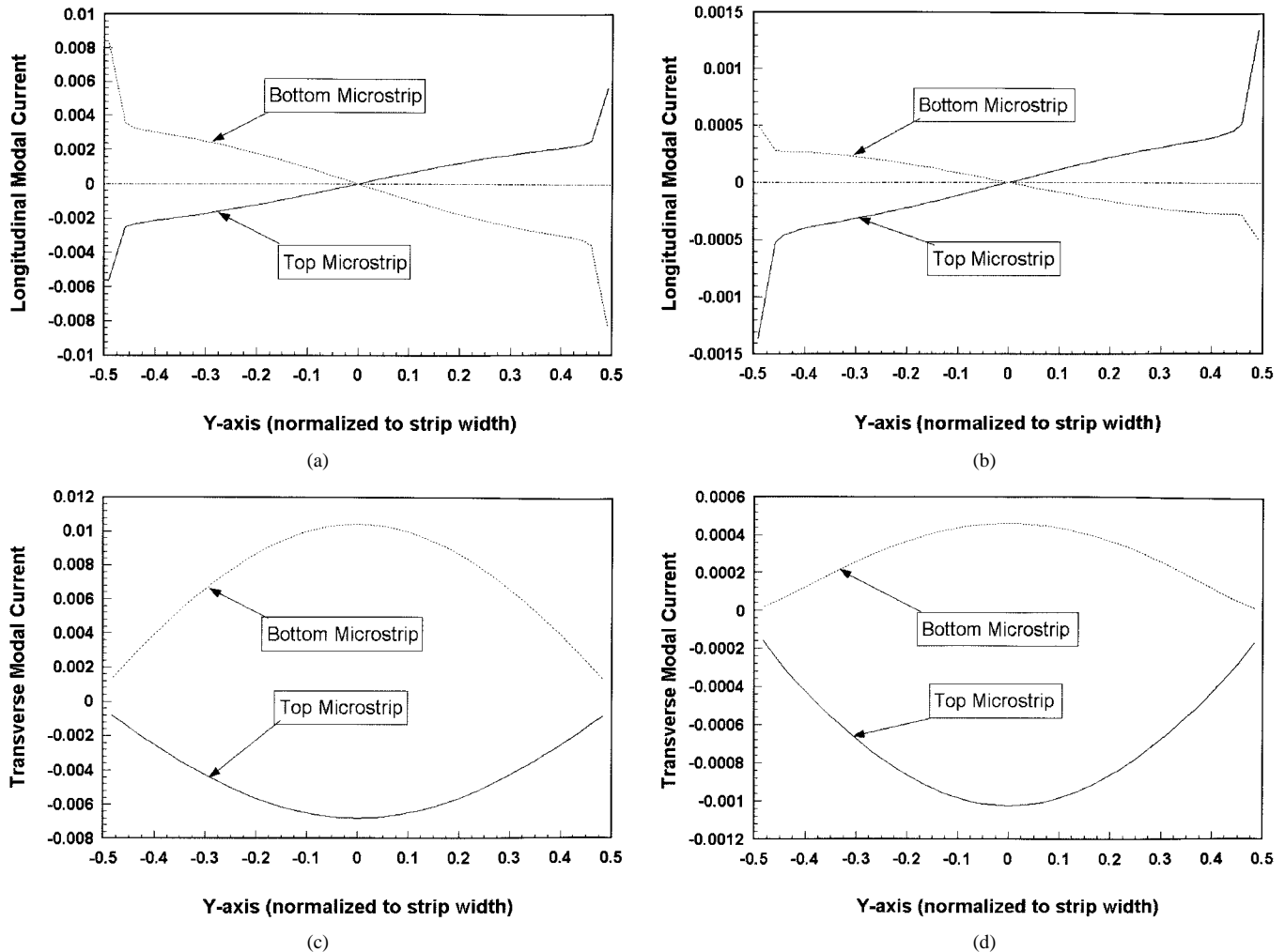


Fig. 4. Modal current distributions of the γ_2 mode on the top (solid line) and bottom (dashed line) microstrips at 31 GHz. The γ_2 modal currents flowing on the top and bottom microstrips are nearly out-of-phase (with a phase difference of 186.1°) and differ in magnitude by a ratio of 0.66:1. (a) The real parts for γ_2 . (b) The imaginary parts for γ_2 . (c) The real parts for γ_2 . (d) The imaginary parts for γ_2 .

vertical central plane (z - x -plane), which is equivalent to a perfect electric conductor (PEC) plane, only the fields on the right half-plane are shown in Figs. 5 and 6.

Fig. 5(a) indicates that the electric field of the γ_1 mode concentrates near the edge of the microstrips. The electric-field lines are directed upwardly and downwardly from the top microstrip. Fig. 5(a) and (b) also reveals that the electric and magnetic fields in the sandwiched dielectric layer (ϵ_{r1}) have smaller amplitudes than those in the bottom dielectric layer (ϵ_{r2}) because the fields induced by the top and bottom strip oppose and reduce each other. However, the total electric field still points downwards since the magnitude of the current flowing on the top-layer strip is greater than that on the bottom-layer strip. In contrast, the electric fields induced by the two microstrips are equally directed in the bottom dielectric layer, such that the total electric field is their sum and is greater than that in the top dielectric layer.

The electric and magnetic fields of the γ_2 mode [see Fig. 6(a) and (b)], however, concentrate in the region sandwiched by the two microstrips. The electric fields emanated from the top microstrip terminate on the bottom microstrip in agreement with the nearly out-of-phase γ_2 modal currents. Applying the image

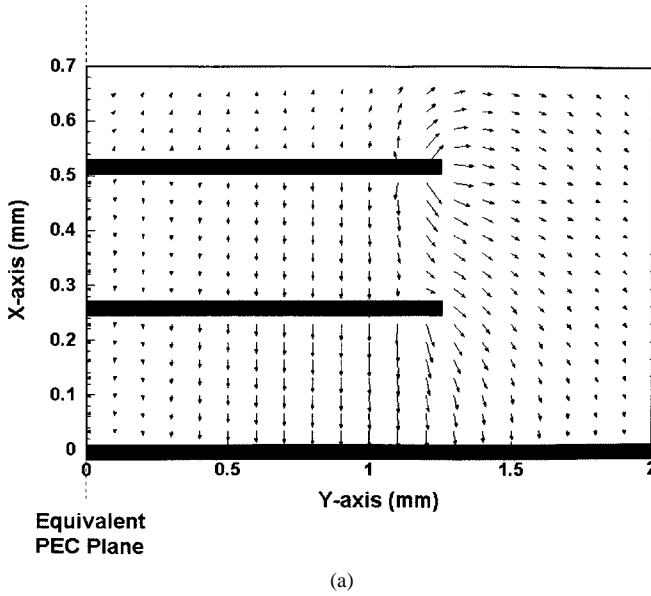
theorem [21], we may insert a PEC plane between the two microstrips without changing in the fields. Careful observation on the transverse fields shown in Fig. 6 reveals that the equivalent PEC approaches the top microstrip, which is equivalent to the reduction of substrate thickness. This is why the dispersion curve of the γ_2 mode moves to higher frequency than that of the γ_1 mode.

III. NARROW-BEAM LEAKY-MODE ANTENNA

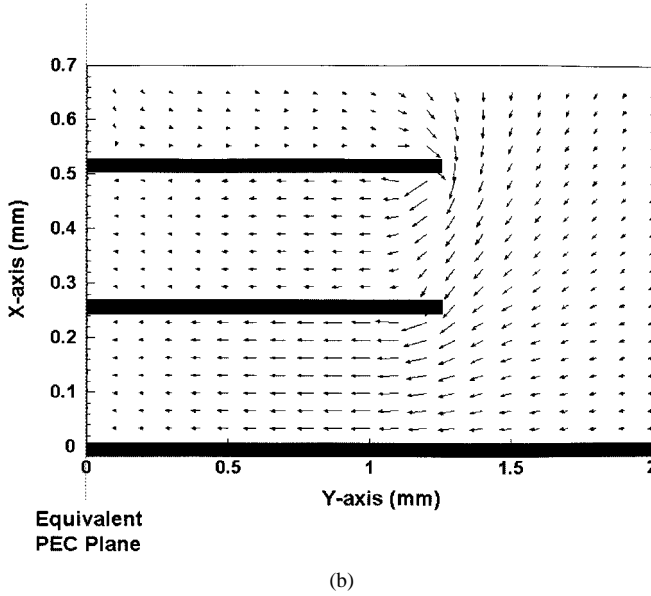
A. Design and Measurement

As stated in Section I, the directivity of the leaky-mode antenna is related to the attenuation constant α . The antenna beamwidth falls and the directivity rises as the attenuation constant decreases. Section II showed that a weakly attenuated leaky mode, i.e., γ_2 , can exist in the two-layer broadside-coupled microstrips. Thus, high-gain leaky-mode antennas can be realized with the γ_2 mode due to the reduction in α .

Experiments are carried out for obtaining the radiation characteristics of the conventional isolated microstrip and the two-layer broadside-coupled microstrips. Firstly, an isolated single-layer microstrip is fabricated as a control experiment.



(a)

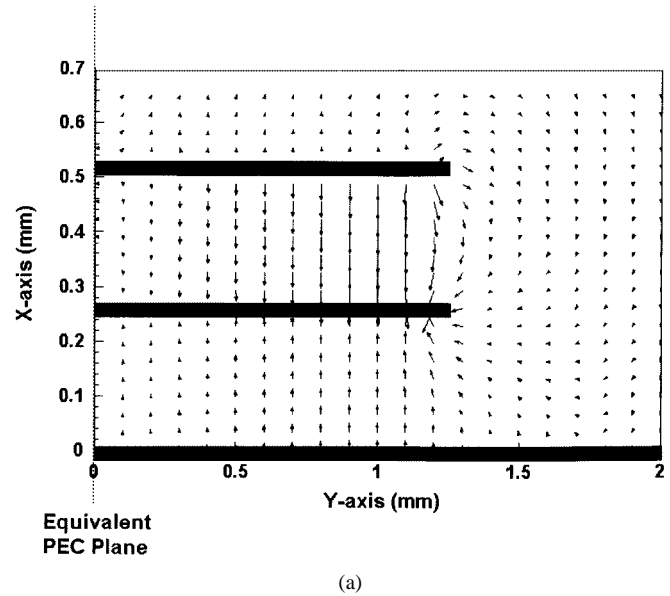


(b)

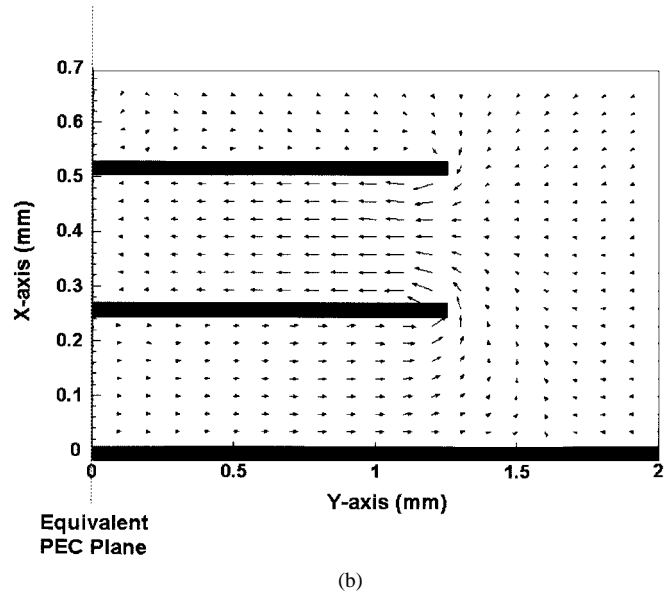
Fig. 5. Transversal: (a) electric E -field and (b) magnetic H -field distributions of the γ_1 leaky mode (approximately in-phase); strong field distribution underneath the bottom microstrip suggests the near in-phase modal current distributions for top and bottom microstrips.

A 50-mm-long microstrip of width 2.5 mm is placed on the 0.254-mm (10-mil)-thick Duroid substrate with relative dielectric constant (ϵ_r) of 3.0. The feeding network consists of a microstrip power divider, followed by two paths made of a $1/4 \lambda_g$ and $3/4 \lambda_g$ lines of appropriate characteristics impedance [22]. The phase difference of the two paths results in 180° out-of-phase at the differential inputs of the leaky line. Thus, the γ_{isol} mode (isolated microstrip with substrate thickness of 0.254 mm), $\gamma_{\text{isol}} = \beta_{\text{isol}} - j\alpha_{\text{isol}}$, is properly excited.

One additional dielectric layer of the same thickness and ϵ_r and a metal strip with the same width are stacked vertically on the isolated microstrip. However, both the top and bottom strips' lengths are greatly extended to be 120 mm since α is reduced after coupling. Care must be exercised to excite the γ_2 mode of Fig. 2. As mentioned in Section I, the two-layer broadside-coupled microstrips shown in Fig. 1 can be considered as the



(a)



(b)

Fig. 6. Transversal: (a) electric and (b) magnetic field distributions of the γ_2 leaky mode (approximately out-of-phase).

simplest three-element Yagi-Uda-like array antenna, including a driver (the bottom microstrip), reflector (the ground plane), and director (the top microstrip). The space distance between the top and bottom microstrips (approximately $0.05 \lambda_g$), however, is much smaller than $\lambda_g/4$ (the regular value between the first reflector and the driver elements of a typical Yagi-Uda antenna array). Consequently, the coupling between the microstrips is much stronger and both of the nearly in-phase (γ_1) and out-of-phase (γ_2) modes could be excited simultaneously by exciting the bottom microstrip only. Applying the well-known even-odd mode analysis, the power ratio of 0.1–0.9 between the γ_1 and γ_2 modes can be obtained. That is, only 10% of the input energy is transferred into the γ_1 mode, which is bound ($\beta/k_0 > 1$) in the operating frequency band of the γ_2 mode, and the power of the γ_1 mode is wasted. In order to reduce the power loss and focus only on the interested γ_2 mode, the designed antenna is directly fed on both microstrips.

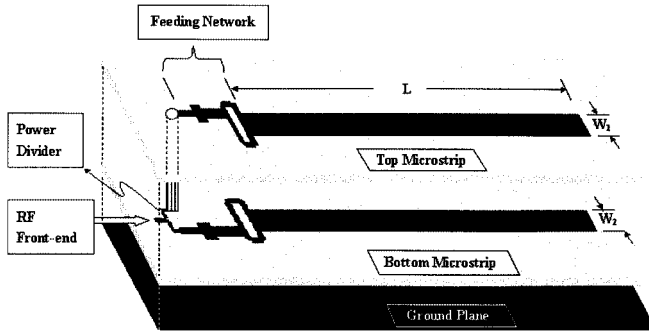


Fig. 7. Layout graph of the reported leaky-mode antenna applying two-layer broadside-coupled microstrips.

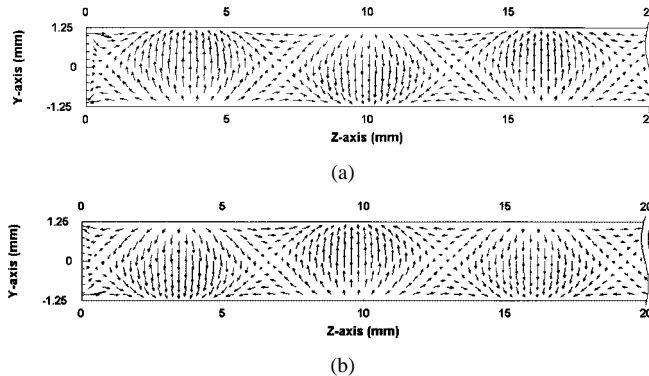


Fig. 8. Simulated modal currents flowing on the: (a) top and (b) bottom microstrip of the reported leaky-wave antenna.

Fig. 7 shows the layout graph of this two-layer structure. A $50\text{-}\Omega$ transmission line is power divided into two paths abiding the power ration of $(0.66)^2$ to excite only the γ_2 mode. The first path is again evenly power divided into two paths of 180° phase difference to excite the bottom microstrip. The second path, while properly designed to support differential inputs at the top microstrip, is further delayed by 186.1° .

Fig. 8 displays the simulation results of the modal currents that flow on the top and bottom microstrips at 35 GHz from the three-dimensional (3-D) commercial software, HFSS of Ansoft. The arrow points to the direction of the current flow and the length of the arrow is directly proportional to the magnitude of the current. Fig. 8 shows only the first 20 mm (approximately $1.5 \lambda_g$) since the leaky-mode antenna is a traveling-wave antenna and the modal currents are distributed periodically along the metal strip, excepting the energy decays exponentially. The distributions of longitudinal (transverse) currents that flow on the two microstrips are both oddly (evenly) symmetric about the $Y = 0$ plane, showing that the first higher order (EH_1) leaky mode is well excited. The currents that flow on the two microstrips are in opposite directions and the magnitude of the current on the bottom microstrip exceeds that on the top microstrip, establishing that the γ_2 mode dominates according to the designed feeding network.

The waves that propagate along the transmission line can be extracted from the modal current distributions in Fig. 8 by invoking the matrix-pencil technique [23]. Four modes, two forward traveling waves γ_1^+, γ_2^+ and their corresponding backward traveling waves γ_1^-, γ_2^- contribute much to the total field, while

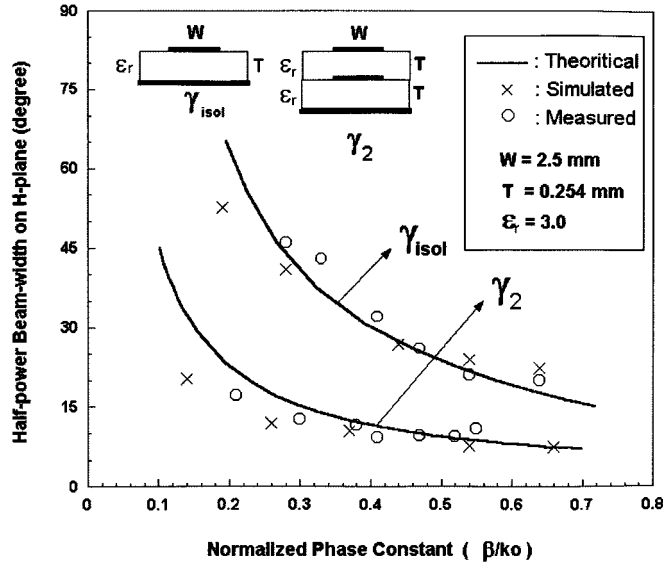


Fig. 9. Theoretical, simulated, and measured half-power beamwidth against normalized phase constants β/k_0 for the leaky-wave antenna applying two-layer broadside-coupled microstrips and the isolated leaky microstrip.

the other modes, such as the bound modes and surface-wave leaky modes, are relatively small in magnitude and are negligible under the excitation. The power ratio of γ_2^+ to γ_2^- is $1:0.11$, showing that the designed antenna can radiate around 89% of the energy into space, of which the value is close to the required 90%, as stated in Section I. If the antenna is longer, the amount of γ_2^- falls, while the aperture efficiency gets a little worse [14]. The normalized phase constants of γ_1^+ and γ_2^+ are 1.04 and 0.67, agreeing closely with the results displayed in Fig. 2. The energy carried by γ_1^+ is found to be only 0.98% of that carried by γ_2^+ ; hence, the γ_2 mode is shown to be dominant in the reported leaky-mode antenna.

Fig. 9 presents the theoretical (full-wave integral-equation method), simulated (HFSS, Ansoft) and measured radiation results. The half-power beamwidth ($\theta_{3\text{dB}}$) on the H -plane (elevation plane or z - x -plane) is plotted against the normalized phase constant β/k_0 to fairly elucidate the gain-enhancement effect. The solid line represents the theoretical result [referring to (1)] and reveals that $\theta_{3\text{dB}}$ decreases as β increases. The \times 's represent the simulated results and the circles represent the measured results. These three results agree closely with each other. Comparing the results for the γ_2 mode with those for the γ_{isol} mode reveals a significant reduction in $\theta_{3\text{dB}}$. The half-power beamwidth of the γ_2 mode is only approximately 40% of that of the γ_{isol} mode over $0.3 < \beta/k_0 < 0.7$.

B. Control of the Attenuation Rate

As mentioned above, a reduction in the attenuation constant α can support a high-gain narrow-beam leaky-mode antenna. It is pointed out in [14] that the decline in α and beamwidth can be related to a thin substrate or one with a low dielectric constant. Finely tuning the thickness or dielectric constant of substrates, however, is difficult, as the microwave substrates are usually made according to commercial specifications. The substrates with quite a thin thickness or low dielectric constant are typically very fragile and expensive. This section shows that the

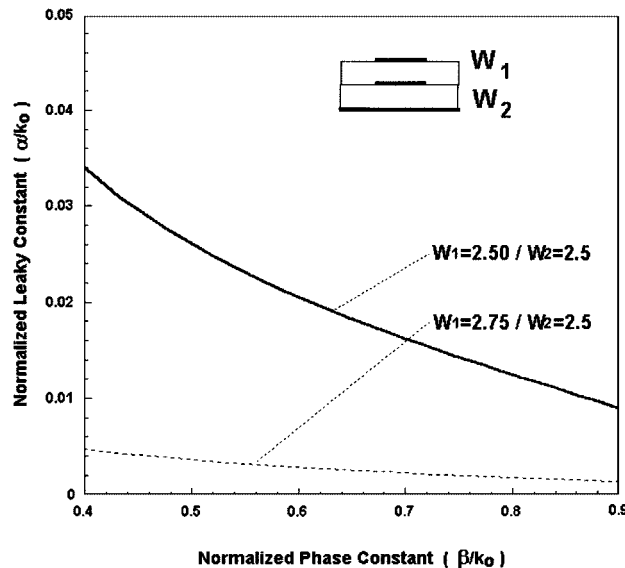


Fig. 10. Normalized attenuation constants α_2/k_0 against normalized phase constants β_2/k_0 of the γ_2 mode due to the variation on W_1 (width of the top microstrip).

attenuation constant α can easily be reduced dramatically by controlling the width of the top microstrip.

Fig. 10 presents the normalized attenuation constant α_2/k_0 of the γ_2 mode (the mode with approximately out-of-phase modal currents) for various W_1 (width of the top microstrip) versus the normalized phase constant β_2/k_0 . The solid line in Fig. 10 represents the case of $W_1 = W_2$ and shows that α_2/k_0 decreases as β_2/k_0 increases. When the width of the top microstrip is increased by 10%, α is lower at a given β , as illustrated by the dashed line in Fig. 10. Restated, the radiation beamwidth can be reduced by adjusting the width of the top microstrip according to (1).

A leaky-mode antenna that employs two-layer broadside-coupled microstrips with a wider top microstrip are designed and measured to demonstrate a further reduction of the beamwidth. The feeding network should be carefully designed to excite the γ_2 mode. The theoretical value (using a two-dimensional (2-D) full-wave integral-equation method) of the normalized attenuation constant α_2/k_0 at 34 GHz is found to be 0.0043, where β_2/k_0 is 0.44 and λ_g is 5.1 mm. The antenna length is 300 mm ($58 \lambda_g$ at 34 GHz), exceeding 217 mm to radiate above 90% of its power. Fig. 11 depicts the measured radiation pattern along the entire elevation plane (H -plane, $\phi = 0$) from -90° to 90° (from the broadside) at 34 GHz. Clearly, since the proposed antenna is long enough to radiate almost all the input energy, no observable back lobe is found in this figure. The measured θ_m (angle of the radiation main beam) is 25.2° , agreeing very closely with the theoretical value 26.1° of θ_m obtained from $\theta_m \approx \sin^{-1}(\beta/k_0)$. The measured half-power beamwidth $\theta_{3\text{dB}}$ is 2.1° at $\theta_m = 25.2^\circ$, also agreeing closely with the theoretical value 1.5° from (1) and much narrower than that of the leaky-mode antenna with equal microstrips ($\theta_{3\text{dB}} = 11.2^\circ$ at $\theta_m = 25.2^\circ$). The result follows the expectation from Fig. 10. An overall efficiency of 81% is measured for the leaky-mode antenna prototype.

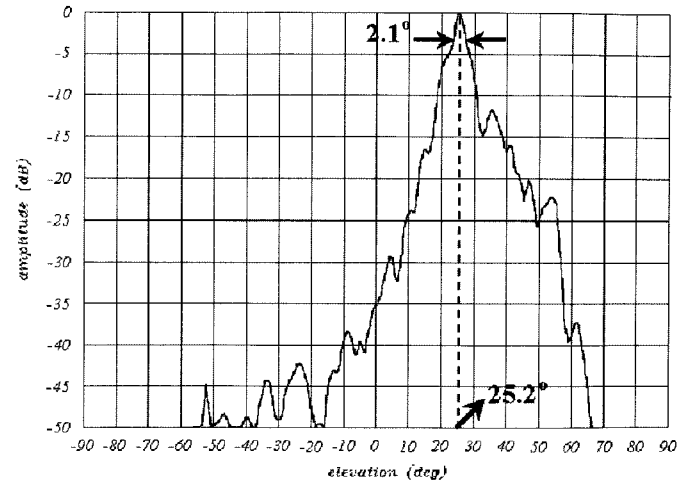


Fig. 11. Measured far-field radiation pattern in the elevation plane (x - z -plane) cut of the reported leaky-mode antenna with a wider top microstrip ($W_1 = 2.75$ mm, $W_2 = 2.5$ mm).

The energy loss mainly comes from the mismatching loss and material losses (conductor loss plus dielectric loss). The return loss is measured to be lower than -15 dB from 32 to 36 GHz showing a bandwidth of 11.8%. However, the material losses are difficult to measure from experiment; hence, only simulation results are mentioned as budget analyses. The conductor (dielectric) loss of the reported electrically long antenna is established to be 8.4% (3.6%), which is the difference between the cases of ideal and actual conductivity (loss tangent). Several measurements show that this antenna can scan from 20° to 40° with $\theta_{3\text{dB}}$ below 5° , establishing that this leaky-mode antenna can scan a very wide range.

IV. CONCLUSION

The higher order leaky modes of broadside-coupled line structures are investigated. Two-layer broadside-coupled microstrip structures are considered, and the dispersion curves, modal currents, and electromagnetic fields are comprehensively discussed. The leaky region of this structure is much broader than that of a conventional isolated microstrip. The coupled EH_1 mode with approximately in-phase modal currents always falls into a lower frequency band and should be treated carefully in practical multilayered microwave integrated circuits (MICs) or monolithic microwave integrated circuits (MMICs).

This paper offers a practical design example of a leaky-mode antenna that invokes the coupled EH_1 mode with approximately out-of-phase modal currents. This weakly attenuated mode can be primarily excited to fabricate a high-gain narrow-beam leaky-mode antenna. However, the attenuation rate can also be increased or decreased over a very wide range by adjusting the ratio of the strips' widths, showing a plain approach to a highly directed antenna, which is important to modern wireless communication systems.

REFERENCES

- [1] J. E. Dalley, "A strip-line directional coupler utilizing a nonhomogeneous dielectric medium," *IEEE Trans. Microwave Theory Tech.*, vol. MTT-17, pp. 706-712, Sept. 1969.

- [2] J. L. Allen, "Broadside-coupled strips in a layered dielectric medium," *IEEE Trans. Microwave Theory Tech.*, vol. MTT-20, pp. 662–669, Oct. 1972.
- [3] P. Bhartia and P. Pramanick, "Computer-aided design models for broadside-coupled striplines and millimeter-wave suspended substrate microstrip lines," *IEEE Trans. Microwave Theory Tech.*, vol. 36, pp. 1476–1481, Nov. 1988.
- [4] Y.-C. Chiang, C.-K. C. Tzuang, and S. Su, "Design of a three-dimensional gap-coupled suspended substrate stripline bandpass filter," *Proc. Inst. Elect. Eng.*, pt. H, vol. 139, no. 4, pp. 376–384, Aug. 1992.
- [5] C.-M. Tsai and K. C. Gupta, "A generalized model for coupled lines and its applications to two-layer planar circuits," *IEEE Trans. Microwave Theory Tech.*, vol. 40, pp. 2190–2199, Dec. 1992.
- [6] F. Tefiku, E. Yamashita, and J. Funada, "Novel directional couplers using broadside-coupled coplanar waveguides for double-sided printed antennas," *IEEE Trans. Microwave Theory Tech.*, vol. 44, pp. 275–282, Feb. 1996.
- [7] L. Carin and N. K. Das, "Leaky waves on broadside-coupled microstrip," *IEEE Trans. Microwave Theory Tech.*, vol. 40, pp. 58–66, Jan. 1992.
- [8] F. J. Villegas, D. R. Jackson, J. T. Williams, and A. A. Oliner, "Leakage fields from planar semi-infinite transmission lines," *IEEE Trans. Microwave Theory Tech.*, vol. 47, pp. 443–454, Apr. 1999.
- [9] K.-F. Huang and C.-K. C. Tzuang, "Leaky modes of vertically stacked microstrips at higher order," in *IEEE MTT-S Int. Microwave Symp. Dig.*, vol. 2, June 2000, Paper WEIF-5, pp. 1077–1080.
- [10] C.-N. Hu and C.-K. C. Tzuang, "Analysis and design of large leaky-mode array employing the coupled-mode approach," *IEEE Trans. Microwave Theory Tech.*, vol. 49, pp. 629–636, Apr. 2001.
- [11] A. A. Oliner and K. S. Lee, "The nature of the leakage from higher modes on microstrip line," in *IEEE MTT-S Int. Microwave Symp. Dig.*, 1986, pp. 55–60.
- [12] W. Menzel, "A new traveling-wave antenna in microstrip," *Arch. Elektr. Übertragung*, vol. 33, pp. 137–140, Apr. 1979.
- [13] Y. Qian, B. C. C. Chang, M. F. Chang, and T. Itoh, "Multi-mode microstrip antennas for reconfigurable aperture," in *IEEE AP-S Symp. Dig.*, vol. 1, 2000, pp. 318–320.
- [14] K. S. Lee, "Microstrip line leaky-wave antenna," Ph.D. dissertation, Polytech. Inst., Brooklyn, NY, 1986.
- [15] D. R. Jackson and A. A. Oliner, "A leaky-wave analysis of the high-gain printed antenna configuration," *IEEE Trans. Antennas Propagat.*, vol. 36, pp. 905–910, July 1988.
- [16] D. R. Jackson, A. A. Oliner, and A. Ip, "Leaky-wave propagation and radiation for a narrow-beam multiple-layer dielectric structure," *IEEE Trans. Antennas Propagat.*, vol. 41, pp. 344–348, Mar. 1993.
- [17] C.-Y. Lee, A. Basu, J. Liao, J. S.-M. Wong, B. Houshmand, and T. Itoh, "Millimeter-wave dielectric leaky-wave antennas," in *Int. Signals, Systems and Electronics Symp.*, 1995, pp. 21–24.
- [18] Y. Wagatsuma, Y. Daicho, and T. Yoneyama, "Millimeter-wave planar antenna for car warning radar," in *Millimeter Waves Topical Symp.*, July 1997, pp. 173–176.
- [19] M. Guglielmi and D. R. Jackson, "Broadside radiation from periodic leaky-wave antennas," *IEEE Trans. Antennas Propagat.*, vol. 41, pp. 31–37, Jan. 1993.
- [20] W. L. Stutzman and G. A. Thiele, *Antenna Theory and Design*. New York: Wiley, 1981, ch. 5, pp. 220–228.
- [21] R. F. Harrington, *Time-Harmonic Electromagnetic Fields*. New York: McGraw-Hill, 1993, ch. 3.
- [22] C.-N. Hu and C.-K. C. Tzuang, "High-efficiency closely coupled microstrip leaky-mode antenna array," in *Asia-Pacific Microwave Conf.*, vol. 1, 1999, pp. 72–75.
- [23] Y. Hua and T. K. Sarkar, "Matrix pencil and system poles," *Signal Process.*, vol. 21, no. 2, pp. 195–198, Oct. 1990.



Kuo-Feng Steve Huang (S'99) was born in Taiwan, R.O.C., on April 26, 1975. He received the B.S. and M.S. degrees in communication engineering from the National Chiao Tung University, Hsinchu, Taiwan, R.O.C., in 1997 and 1999, respectively, and is currently working toward the Ph.D. degree at the National Chiao Tung University.

His current research interests include electromagnetic-field theory analysis and its application on designing leaky-mode antennas.



Ching-Kuang C. Tzuang (S'80–M'80–SM'92–F'99) received the B.S. degree in electronic engineering from the National Chiao Tung University, Hsinchu, Taiwan, R.O.C., in 1977, the M.S. degree from the University of California at Los Angeles, in 1980, and the Ph.D. degree in electrical engineering from the University of Texas at Austin, in 1986.

From 1981 to 1984, he was with TRW, Redondo Beach, CA, where he was involved with analog and digital MMICs. Since 1986, he has been with the Institute of Communication Engineering, National Chiao Tung University. His research activities involve the design and development of millimeter-wave and microwave active and passive circuits and the field theory analysis and design of various complex waveguiding structures and large-array antennas. He has supervised 58 M.S. students and 15 Ph.D. students.

Dr. Tzuang helped in the formation of the IEEE Microwave Theory and Techniques Society (IEEE MTT-S) Taipei chapter, and served as secretary, vice chairman, and chairman in 1988, 1989, and 1990, respectively. He has been on the Asia-Pacific Microwave Conference International Steering Committee, where, since 1994, he has represented the Taipei chapter as the international liaison officer.